

Ca²⁺ signaling in mouse mesenteric small arteries: myogenic tone and adrenergic vasoconstriction

Joseph Zacharia, Jin Zhang, and W. Gil Wier

Department of Physiology, School of Medicine, University of Maryland, Baltimore, Maryland

Submitted 23 June 2006; accepted in final form 10 November 2006

Zacharia J, Zhang J, Wier WG. Ca²⁺ signaling in mouse mesenteric small arteries: myogenic tone and adrenergic vasoconstriction. *Am J Physiol Heart Circ Physiol* 292: H1523–H1532, 2007. First published November 17, 2006; doi:10.1152/ajpheart.00670.2006.—Arteries that have developed myogenic tone (MT) are in a markedly different physiological state compared with those that have not, with higher cytosolic [Ca²⁺] and altered activity of several signal transduction pathways. In this study, we sought to determine whether α_1 -adrenoceptor-induced Ca²⁺ signaling is different in pressurized arteries that have spontaneously developed MT (the presumptive physiological state) compared with those that have not (a common experimental state). At 32°C and intraluminal pressure of 70 mmHg, cytoplasmic [Ca²⁺] was steady in most smooth muscle cells (SMCs). In a minority of cells (34%), however, at least one propagating Ca²⁺ wave occurred. α_1 -Adrenoceptor activation (phenylephrine, PE; 0.1–10.0 μ M) caused strong vasoconstriction and markedly increased the frequency of Ca²⁺ waves (in virtually all cells). However, when cytosolic [Ca²⁺] was elevated experimentally in these arteries ([K⁺] 20 mM), PE failed to elicit Ca²⁺ waves, although it did elevate [Ca²⁺] (F/F₀) further and caused further vasoconstriction. During development of MT, the cytosolic [Ca²⁺] (F/F₀) in individual SMCs increased, Ca²⁺ waves disappeared (from SMCs that had them), and small Ca²⁺ ripples (frequency \sim 0.05 Hz) appeared in \sim 13% of cells. PE elicited only spatially uniform increases in [Ca²⁺] and a smaller change in diameter (than in the absence of MT). Nevertheless, when cytosolic [Ca²⁺] and MT were decreased by nifedipine (1 μ M), PE did elicit Ca²⁺ waves. Thus α_1 -adrenoceptor-mediated Ca²⁺ signaling is markedly different in arteries with and without MT, perhaps due to the elevated [Ca²⁺], and may have a different molecular basis. α_1 -Adrenoceptor-induced vasoconstriction may be supported either by Ca²⁺ waves or by steady elevation of cytoplasmic [Ca²⁺], depending on the amount of MT.

phenylephrine; confocal microscopy; calcium waves; smooth muscle; imaging

CONTRACTION OF VASCULAR SMOOTH MUSCLE in response to neurotransmitters and hormones involves changes in both intracellular [Ca²⁺] and diverse signal transduction pathways that influence ion channels, protein kinases, phosphatases, second messengers, and other enzymes (for review, see Ref. 35). The characteristics of the spatial and temporal patterns of the changes in [Ca²⁺] are expected to be of fundamental importance in determining their efficacy in activating contraction, through Ca²⁺/calmodulin-dependent myosin light chain kinase (MLCK). In many types of arteries, and in some veins, activation of α_1 -adrenoceptors of isolated small arteries elicits propagating Ca²⁺ waves that occur asynchronously in the individual smooth muscle cells (SMCs; for review, see Ref.

18). It has been suggested that such asynchronous Ca²⁺ waves, which arise from Ca²⁺ released through inositol 1,4,5-trisphosphate receptors (InsP₃R), are highly efficient in delivering Ca²⁺ to MLCK that is tethered to the contractile myofilaments (20). In some small arteries, a different type of contractile Ca²⁺ signal also may be generated, particularly when levels of receptor activation are high: Ca²⁺ oscillations that are spatially uniform and synchronized among the different cells (6, 23). The asynchronous Ca²⁺ waves, which are dependent on InsP₃R (16, 22), generate steady overall vasoconstriction, whereas the synchronous Ca²⁺ oscillations generate oscillatory vasomotion (referred to as “adrenergic vasomotion”) (for review, see Ref. 26). These concepts have been developed largely as a result of the ability to obtain spatially resolved observations of intracellular [Ca²⁺] with fluorescent Ca²⁺ indicators within individual SMC of the blood vessel wall (24). When internally pressurized, many types of small arteries also develop myogenic tone (MT), known to be an important determinant of total vascular resistance. MT is dependent on changes of intracellular [Ca²⁺] (15, 27) but also, importantly, involves increased activity of certain protein kinases, possible transactivation of extracellular growth factor receptor, activity of the local renin-angiotensin system (RAS), and other enzymes (for review on mechanisms of MT, see Ref. 7). Surprisingly, however, it was not known previously whether α_1 -adrenoceptor-induced Ca²⁺ signals in such arteries were of the type described above or whether they might be different, due to the markedly different state of the cell once MT has developed. The only previous study in which spatially resolved Ca²⁺ imaging was performed in small arteries that had MT (24) was complicated by the development of adrenergic vasomotion, preventing the clear observation of Ca²⁺ signaling in individual SMC. Similarly, the changes in [Ca²⁺] that might occur within individual SMCs during development of myogenic tone had not been resolved previously with confocal imaging. In the present study, therefore, we sought to observe, in individual SMCs of intact pressurized arteries at 32°C, the changes in [Ca²⁺] that occur during development of MT and to observe the changes in [Ca²⁺] elicited by activation of α_1 -adrenoceptors before and after MT developed. We studied mouse mesenteric small arteries pressurized at 70 mmHg. These arteries developed MT but did not usually develop oscillatory vasomotion in response to α_1 -adrenoceptor agonists, thus facilitating spatially resolved observations of intracellular Ca²⁺ in individual SMCs. The major result is that α_1 -adrenoceptor agonists induce mainly an increase in “global” [Ca²⁺] after MT has developed fully, and they induce asynchronous propagat-

Address for reprint requests and other correspondence: W. G. Wier, Dept. of Physiology, Univ. of Maryland, 655 West Baltimore St., Baltimore, MD 21201 (e-mail: gwier001@umaryland.edu).

The costs of publication of this article were defrayed in part by the payment of page charges. The article must therefore be hereby marked “advertisement” in accordance with 18 U.S.C. Section 1734 solely to indicate this fact.

ing Ca^{2+} waves only when MT has not developed or when Ca^{2+} influx is reduced experimentally. We present evidence that the switch from asynchronous propagating Ca^{2+} waves to simple increases in global $[\text{Ca}^{2+}]_i$ is, in fact, related to the increase in cytosolic $[\text{Ca}^{2+}]_i$ and/or Ca^{2+} influx.

METHODS

All protocols were reviewed and approved by the Institutional Animal Care and Use Committee of the University of Maryland, School of Medicine. Mice were maintained on 12:12-h light-dark schedule at 22–25°C and 45–65% humidity and were fed ad libitum on a standard rodent diet and tap water. Adult mice (22–35 g, 12–18 wk old), were killed with CO_2 . The mesenteric arcade was dissected from the abdominal cavity, rinsed free of blood, and placed in a temperature-controlled dissection chamber (5°C) containing a dissection solution of the following composition (in mmol/l): 3.0 MOPS, 145.0 NaCl, 5.0 KCl, 2.5 CaCl_2 , 1.0 MgSO_4 , 1.0 KH_2PO_4 , 0.02 EDTA, 2.0 pyruvate-Na, and 5.0 glucose (pH 7.4).

Loading of resistance arteries with calcium indicators. Isolated arteries were dissected using methods similar to those described previously (4). Dissected segments of the third-order arteries, 1–2 mm in length, were transferred to a recording chamber, where their ends were mounted on glass pipettes (tip diameter 60–100 μm) and secured by 10-0 Ethilon ophthalmic nylon sutures (Ethicon, Somerville, NJ). One pipette was attached to a servo-controlled pressure-regulating device (Living Systems, Burlington, VT), whereas the other was attached to a closed stopcock to study the pressure-dependent effects in the absence of intraluminal flow. The vessel was then loaded with a calcium indicator in dissection solution containing fluo-4 AM at 15 μM , 1.5% (vol/vol) DMSO, and 0.03% (vol/vol) cremophor EL. Loading was allowed to proceed for 3 h at room temperature with the intraluminal pressure set to 70 mmHg. Soon after loading, the arteries were continuously superfused with gassed Krebs solution containing (in mmol/l) 112.0 NaCl, 25.7 NaHCO_3 , 4.9 KCl, 2.0 CaCl_2 , 1.2 MgSO_4 , 1.2 KH_2PO_4 , 11.5 glucose, and 10.0 HEPES (pH 7.4, gas composition 5% O_2 -5% CO_2 -90% N_2). During the entire process, the arteries that developed significant leaks were discarded.

Measurement and analysis of fluorescence and arterial diameter. For two-dimensional confocal imaging, we used a “real-time” confocal imaging system (Solamere Technology Group, Salt Lake City, UT) consisting of a Yokogawa confocal scanner (model CSU10) and an intensified charge-coupled device camera (model XR/Mega-10). This produced 30 images/s, and images of $75 \times 50 \mu\text{m}$ were collected. The confocal imaging system utilized a Nikon inverted microscope equipped with a “water” objective lens ($\times 60$; numerical aperture 1.2). A water objective was used to obtain adequate working distance, as described previously (24). “Radial” confocal sections were used to image SMCs in cross section during active contractions (23). Individual SMCs can be successfully “tracked” during vasomotion by using radial sections. Measurements of the arterial wall position obtained from the confocal setup were done by using the edges of the fluorescence image recorded at 2 frames/s. For analyzing calcium sparks (30 frames/s) and calcium transients when fully contracted with phenylephrine (PE; 2 frames/s), “tangential” sections were used in arteries loaded with fluo-4. Although we may refer to the images as “ Ca^{2+} images,” all the images are simply those of Ca^{2+} -dependent fluo-4 fluorescence. Autofluorescence was negligible in arteries in these experiments. Measurements of arterial wall position from transmitted light images (in arteries not loaded with fluo-4) were recorded at 2 images/s with a Nikon $\times 20$ objective.

Images were analyzed using custom software written with IDL (Interactive Data Language, version 6.3; Research Systems, Boulder, CO). This software was used to obtain average fluorescence from areas of interest (AOIs) within the images. Where appropriate, F/F_0 was calculated. SigmaPlot 2004 (version 9.0; SPSS, St. Louis, MO) and GraphPad Prism (version 3.0; San Diego, CA) analysis software

were used to graph the data. IDL was used to calculate power spectra, as described in more detail below (see RESULTS). Two quantities were typically derived from the movies of arterial wall fluorescence and presented in bar graphs: 1) the percentage of cells that produced (at least 1) propagating Ca^{2+} wave during a recording period of 250 s and 2) the average frequency of such waves in each cell. Mean values and standard errors of the mean (SE) under a particular experimental condition were obtained by pooling the data from ~ 25 cells from each of several different arteries (3 to 6) in which the same experiment was performed.

Drugs and solutions. PE, $[\text{Sar}_1, \text{Ile}_8]$ -ANG II, and nifedipine were prepared as concentrated stock solutions and diluted in the superfusate reservoir. PE, $[\text{Sar}_1, \text{Ile}_8]$ -ANG II, and nifedipine were obtained from Sigma Chemical (St. Louis, MO); fluo-4 AM was purchased from Molecular Probes (Eugene, OR). The selective Rho-kinase inhibitor Y-27632 [(+)-(R)-*trans*-4-(1-aminoethyl)-(4-pyridyl)cyclohexanecarboxamide dihydrochloride] was purchased from Calbiochem. In the experiments in which a “zero”-calcium solution was used, the solution had the same composition as the standard Krebs with the omission of CaCl_2 and the addition of Na_2EGTA (1 mM). In the experiments in which high-potassium solutions were used, NaCl was replaced by KCl on a mole-for-mole basis.

RESULTS

MT and adrenergic vasoconstriction at 32°C. Arteries were initially pressurized at 70 mmHg at room temperature (21–23°C). The experiment began when temperature was raised to 32°C. MT then developed (Fig. 1A, arrow), but typically with a delay (latency period) ranging from 10 to 30 min, similar to that reported previously (27). This brief latency period provided the opportunity to examine Ca^{2+} and adrenergic responses in the absence of MT but at near-mammalian temperature and at physiological transmural pressure.

During the latency period before MT, PE at concentrations of 0.1, 1.0, and 10.0 μM elicited strong vasoconstriction (Fig. 1B). MT then often developed or augmented abruptly (Fig. 1B, second arrow). After full development of MT, the same concentrations of PE elicited contractions that were approximately one-half those before MT (or none at all, if the artery was already contracted to a greater level than reached before, as at 0.1 μM PE in the example shown). Although the change in diameter was smaller, the final diameter reached at 1.0 and 10.0 μM PE was nevertheless usually virtually identical before and after MT had developed. In five arteries, 1.0 μM PE produced constriction to $60 \pm 3\%$ of passive diameter before MT and to $59 \pm 3\%$ of passive diameter after MT. In three arteries, 10.0 μM PE produced constriction to $67 \pm 1\%$ of passive diameter before MT and to $65 \pm 2\%$ of passive diameter after MT. Thus MT strongly influences responses to α_1 -adrenoceptor agonists in terms of the change in diameter, although, remarkably, the final diameter reached is the same (Fig. 1B).

Intracellular Ca^{2+} before, during, and after development of MT. Before examining any differences that might exist in agonist-induced Ca^{2+} signaling between arteries that have developed MT and those that have not, we first sought to observe intracellular $[\text{Ca}^{2+}]_i$ within individual SMCs before, during, and after development of MT. At 32°C and 70 mmHg, before the spontaneous development of MT, $[\text{Ca}^{2+}]_i$ was quite variable in different SMCs (Fig. 2, Aa, Ab, and Ba). In most SMCs, intracellular $[\text{Ca}^{2+}]_i$ was relatively constant, but in

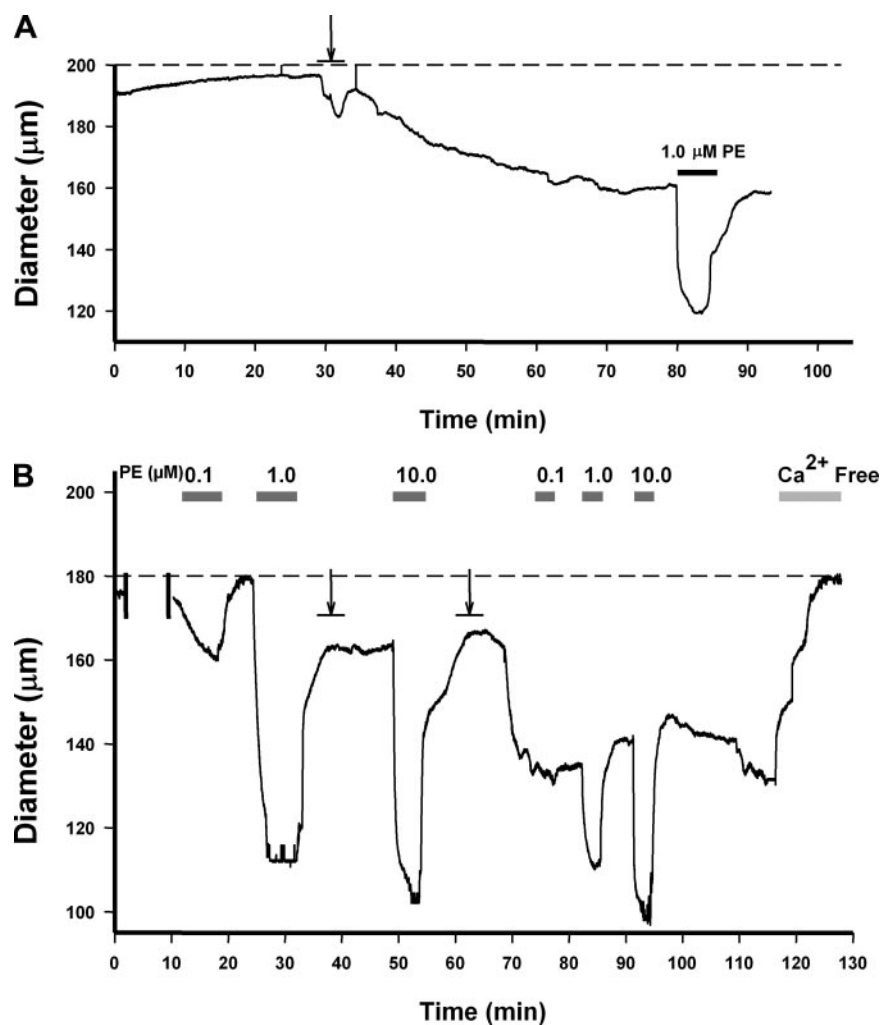


Fig. 1. Spontaneous development of myogenic tone (MT) and vasoconstriction in response to α_1 -adrenoceptor activation before and after development of MT. *A*: continuous recording of diameter of a mouse mesenteric small artery at a transmural pressure of 70 mmHg and a temperature of 32°C. MT begins to develop spontaneously at time indicated by arrow. After MT developed, phenylephrine (PE; 1.0 μ M) was applied. *B*: dose-response to PE (0.1, 1.0, and 10.0 μ M) before and after spontaneous development of MT. MT developed partially (1st arrow) and then abruptly and completely (2nd arrow). Shaded bars indicate periods in which PE was present. After full development of MT, PE at 0.1 μ M did not cause further vasoconstriction, and at 1.0 and 10.0 μ M, PE caused smaller constrictions than before MT. Ca^{2+} -free external solution was applied at the end of the experiment to determine the passive diameter (PD) and the amount of MT [28% in this case: $(\text{PD} - \text{MT})/\text{PD} = (180 \mu\text{m} - 130 \mu\text{m})/180 \mu\text{m}$].

others, spontaneous propagating Ca^{2+} waves and local Ca^{2+} transients of various amplitudes were readily apparent (e.g., Fig. 2*Ba*, red trace; see “before_tone” movie in supplementary data). (The online version of this article contains supplemental data.) Ca^{2+} sparks, which are readily quantifiable because of their spatiotemporal characteristics, occurred at a rate of 0.116 ± 0.010 sparks \cdot s $^{-1}$ \cdot cell $^{-1}$ ($n = 3$ arteries). Large Ca^{2+} waves also were readily identifiable and were quantified before and after development of MT (described below).

MT develops spontaneously, and this event is preceded by the beginning of the rise in arterial wall $[\text{Ca}^{2+}]$ (27). During this time, the fluorescence in some, but not all, individual SMCs, rose smoothly (Fig. 2, *Ac*, *Ad*, and *Bb*). Because there was little or no movement early during this event, the images in Fig. 2, *Aa* and *Ac*, are from the same SMC, obtained without adjusting the focus of the microscope. In 21 cells from 3 arteries in which the same individual SMCs could be identified (as in Fig. 2), the normalized minimum fluorescence ratio (F/F_0 ; pseudoratio) within an AOI from the same cell increased from 1.0 to 2.090 ± 0.097 . The minimum value during the recording period was used so that Ca^{2+} waves or spikes did not affect the estimate of F_0 or F . As is clear from Fig. 2*Bb*, the Ca^{2+} waves ceased in most cells in which $[\text{Ca}^{2+}]$ rose. A few cells continued to produce Ca^{2+} waves. Overall (5 arteries, 115

cells), however, the percentage of cells producing Ca^{2+} waves (at least 1 during 225 s) declined from 34.5 ± 2.5 to 1.8 ± 1.1 (Fig. 2*Ca*).

Other variable, spontaneous smaller fluctuations of intracellular $[\text{Ca}^{2+}]$ occurred frequently, however, particularly before MT developed. For example, the cell shown by the blue trace in Fig. 2*Ba* produced small fluctuations that are neither Ca^{2+} waves nor Ca^{2+} sparks. This type of Ca^{2+} signaling is not easily categorized. Instead of attempting such categorization, we characterized the fluctuations in fluorescence by calculating the fluorescence power spectra in a small AOI (1.0 μm^2) of each individual cell (~ 25) visible in the optical section. These individual power spectra were then averaged to obtain an average spectrum, as shown in Fig. 2*Da*. The average power spectrum showed substantially increased power (compared with $1/f$ power) over the range of 0.02 to 0.1 cycles/s. The large Ca^{2+} waves observed in some cells (red trace, Fig. 2*Ba*) occurred at a frequency of ~ 0.04 cycles/s, within the broadly elevated region of the power spectrum. Power spectra measured during development of MT (Fig. 2*Db*) showed a general decrease in power over the frequency range, 0.02 to 1.0 Hz, with the difference being maximal at ~ 0.04 Hz. This is similar to the frequency of the large Ca^{2+} waves observed in many cells before MT (Fig. 2*Cb*) and also shows that development of

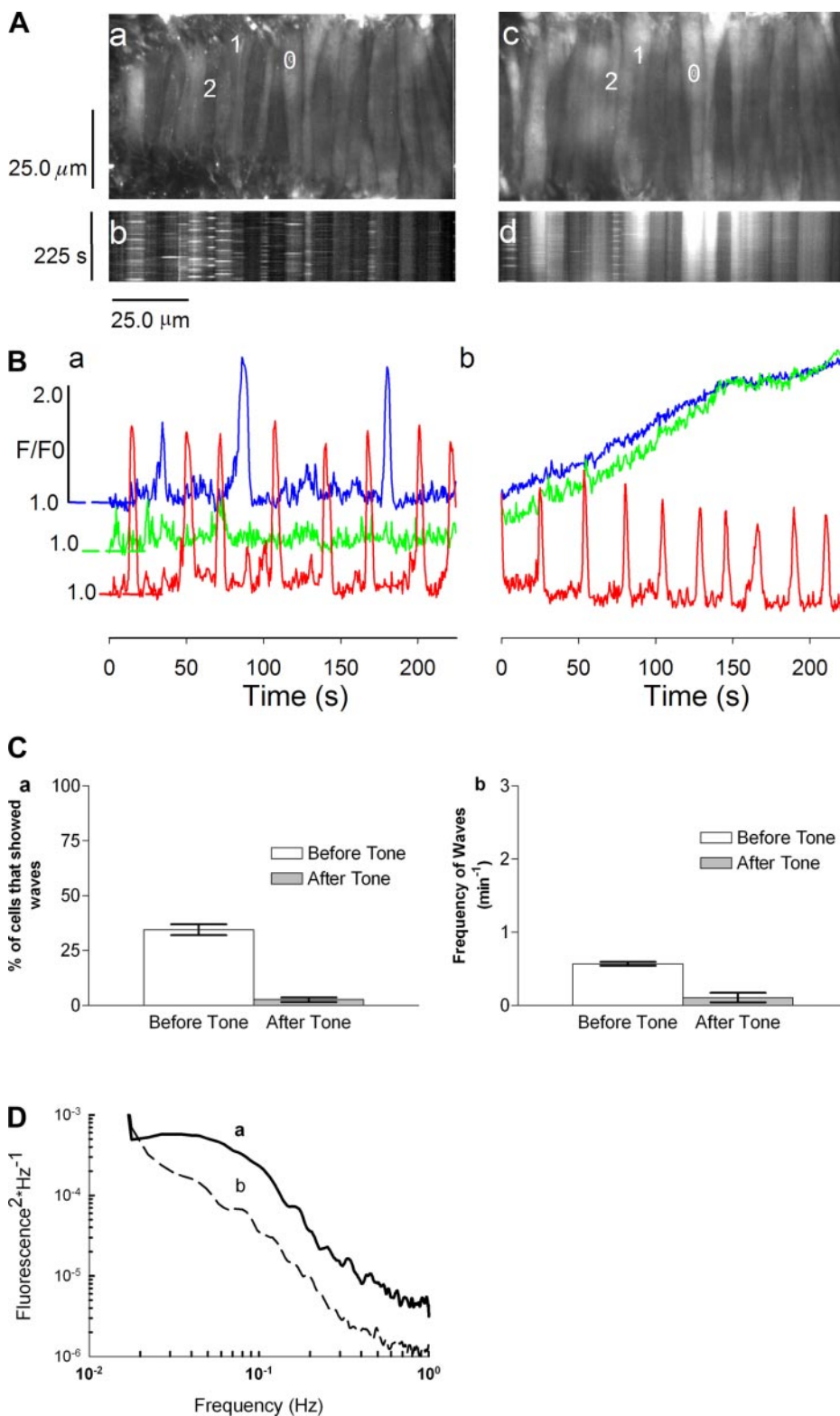


Fig. 2. As MT develops, cytoplasmic $[Ca^{2+}]$ rises and Ca^{2+} waves in individual smooth muscle cells (SMCs) become less frequent. *A*: averaged confocal images of fluo-4 fluorescence in media of artery (*a* and *c*) and virtual line-scan images (*b* and *d*) obtained from 450 frames. Frame rate, 2 s^{-1} . *Ba*: tracings of fluo-4 fluorescence from 3 selected areas of interest (AOIs; $1.0\ \mu\text{m}^2$), indicated as 0 (blue), 1 (green), and 2 (red) in *A*. Traces are “pseudoratio” F/F_0 . *Bb*: same SMCs as in *A* during spontaneous development of MT. AOIs are not exactly the same because of some movement. *C*: percentage of SMCs producing spontaneous Ca^{2+} waves (*a*) and their frequency (*b*) before and after MT (5 arteries, 115 cells). *D*: fluorescence power spectra derived from AOIs in 25 cells before (*a*) and during (*b*) development of MT. Development of MT is associated with a large decrease in fluorescence (i.e., $[Ca^{2+}]$) fluctuations over the frequency range from 0.02 to 0.10 Hz.

MT is accompanied by cessation of this type of Ca^{2+} fluctuation. Fluorescence power spectra (Fig. 2D) contain much more information than the simple measurements of the “average” Ca^{2+} wave frequency (Fig. 2Cb), although mechanistic information on the Ca^{2+} fluctuations that are not waves is still lacking.

As just described, large spontaneous, propagating asynchronous Ca^{2+} waves were virtually never observed in the arteries that had fully developed MT. Nevertheless, some arteries (Fig. 3, *Aa*, *Ab*, and *Ba*) but not others (Fig. 3, *Ac*, *Ad*, and *Bb*) produced relatively small, somewhat irregular fluctuations in fluorescence. These appeared similar to the “ Ca^{2+} ripples”

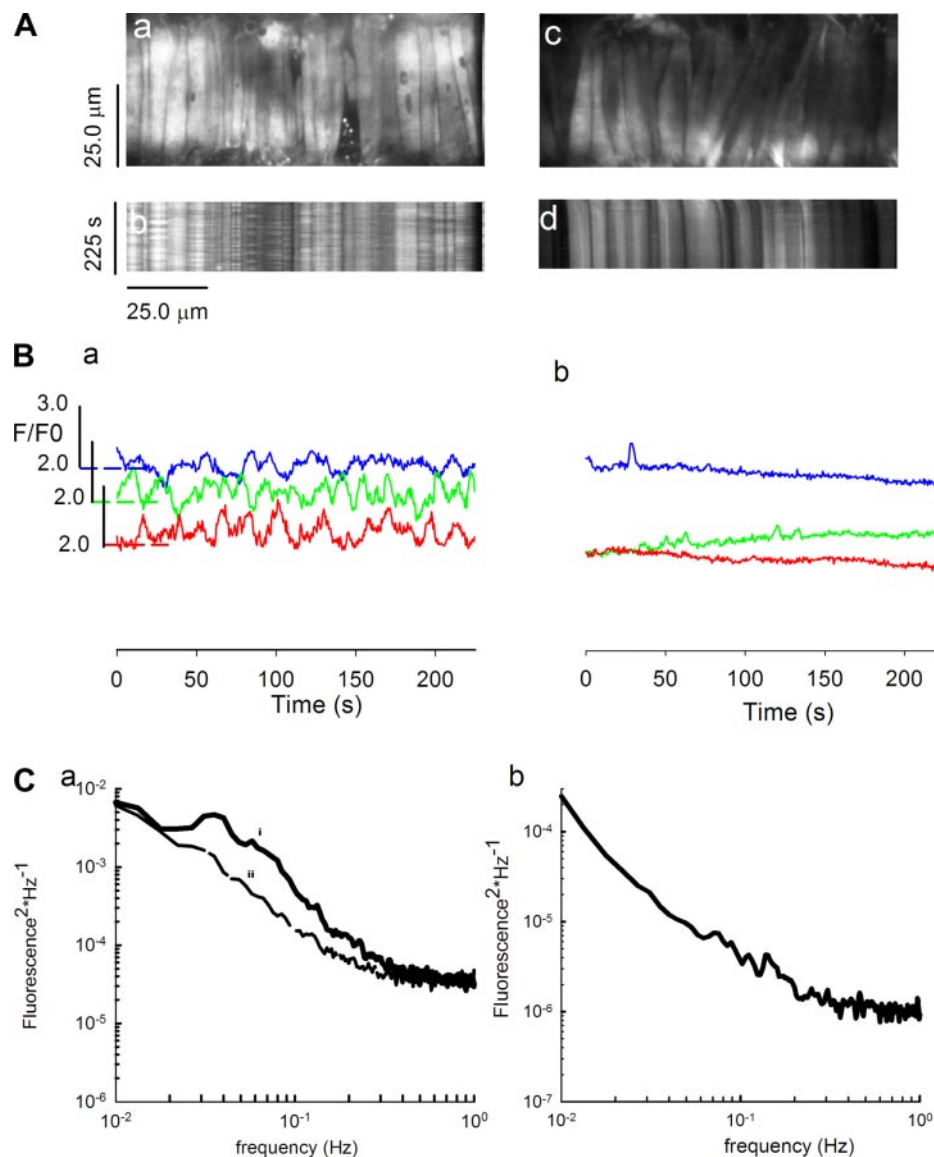


Fig. 3. Ca^{2+} ripples in arteries with MT. In 13% of SMCs in arteries with MT, Ca^{2+} ripples are present and can be abolished by the competitive angiotensin II antagonist $[\text{Sar}_1, \text{Ile}_8]\text{-ANG II}$. *A*: ripples are present in the artery shown in *a* and *b*; ripples are absent in the artery shown in *c* and *d*. Averaged confocal images of fluo-4 fluorescence in media of artery are shown at *top*, and virtual line-scan images are shown at *bottom*. Frame rate, 2 s^{-1} . *B*: tracings of fluo-4 fluorescence from 3 selected AOIs ($1.0 \mu\text{m}^2$) in SMCs in artery with (*a*) and without ripples (*b*). *C*: fluorescence power spectra derived from AOIs in 25 cells before (*i*) and after (*ii*) application of $[\text{Sar}_1, \text{Ile}_8]\text{-ANG II}$ (10 nM) (*a*) and fluorescence power spectra derived from AOIs in 25 cells that did not have ripples (*b*).

(Fig. 3*Ba*) reported previously in rat tail artery (1) and that have been attributed to activity of the intrinsic RAS system. Indeed, the angiotensin II competitive antagonist $[\text{Sar}_1, \text{Ile}_8]\text{-ANG II}$ (10 nM) abolished the ripples and caused a $9 \pm 1\%$ decrease in MT. Analysis of power spectra of the fluorescence (as described above) showed that fluctuations at 0.04 Hz were most sensitive to the angiotensin antagonist (Fig. 3*Ca*). Thus a small component of MT in some mouse arteries appears to be maintained by the local RAS, as in rat tail arteries. The conditions or factors that allow some arteries, but not others, to produce ripples are not known. The majority of mouse arteries did not show such Ca^{2+} ripples, however, and evidence of them was not seen in line-scan images (Fig. 3*Ad*), AOI traces (Fig. 3*Bb*), or power spectra (Fig. 3*Cb*).

α_1 -Adrenergic Ca^{2+} signaling. Before the spontaneous development of MT, the mouse arteries contracted strongly in response to the α_1 -adrenoceptor agonists (PE) (Fig. 1). The Ca^{2+} signaling elicited by PE under this condition (Fig. 4*A*; see “10PE_before_tone” movie in supplemental data) was similar to that we and others have reported previously for rat mesen-

teric small arteries (23, 28, 36), rabbit inferior vena cava (21, 30), rat tail artery (1, 8), and rat cerebral small artery (11). Briefly, upon exposure to PE (1–10 μM), most vascular SMCs in the mouse mesenteric small arteries produced asynchronous propagating Ca^{2+} waves, with the numbers of cells producing Ca^{2+} waves and the frequency of the Ca^{2+} waves being a function of the [PE] (Fig. 4*C*). At a concentration of 1.0 μM , PE elicited (at least 1) Ca^{2+} wave in $72 \pm 6\%$ of cells (5 arteries), and the mean frequency of the waves in these cells was $1.92 \pm 0.13 \text{ min}^{-1}$ (Fig. 4*C*). In these same five arteries, 10.0 μM PE elicited Ca^{2+} waves in $87 \pm 5\%$ of the cells, and the mean frequency of the waves was $2.44 \pm 0.11 \text{ min}^{-1}$ (Fig. 4*C*). Although the frequency of the waves elicited by PE was actually similar to what occurs spontaneously in some cells (e.g., Fig. 2*Ba*), the fraction of cells that produce such waves is greatly increased by PE.

Once arteries had developed MT, however, the response to α_1 -adrenoceptor agonists was fundamentally different than before, as shown in Fig. 4, *Ba* (1.0 μM PE) and *Bb* (10.0 μM PE) (see “10PE_after_tone” movie in supplementary data).

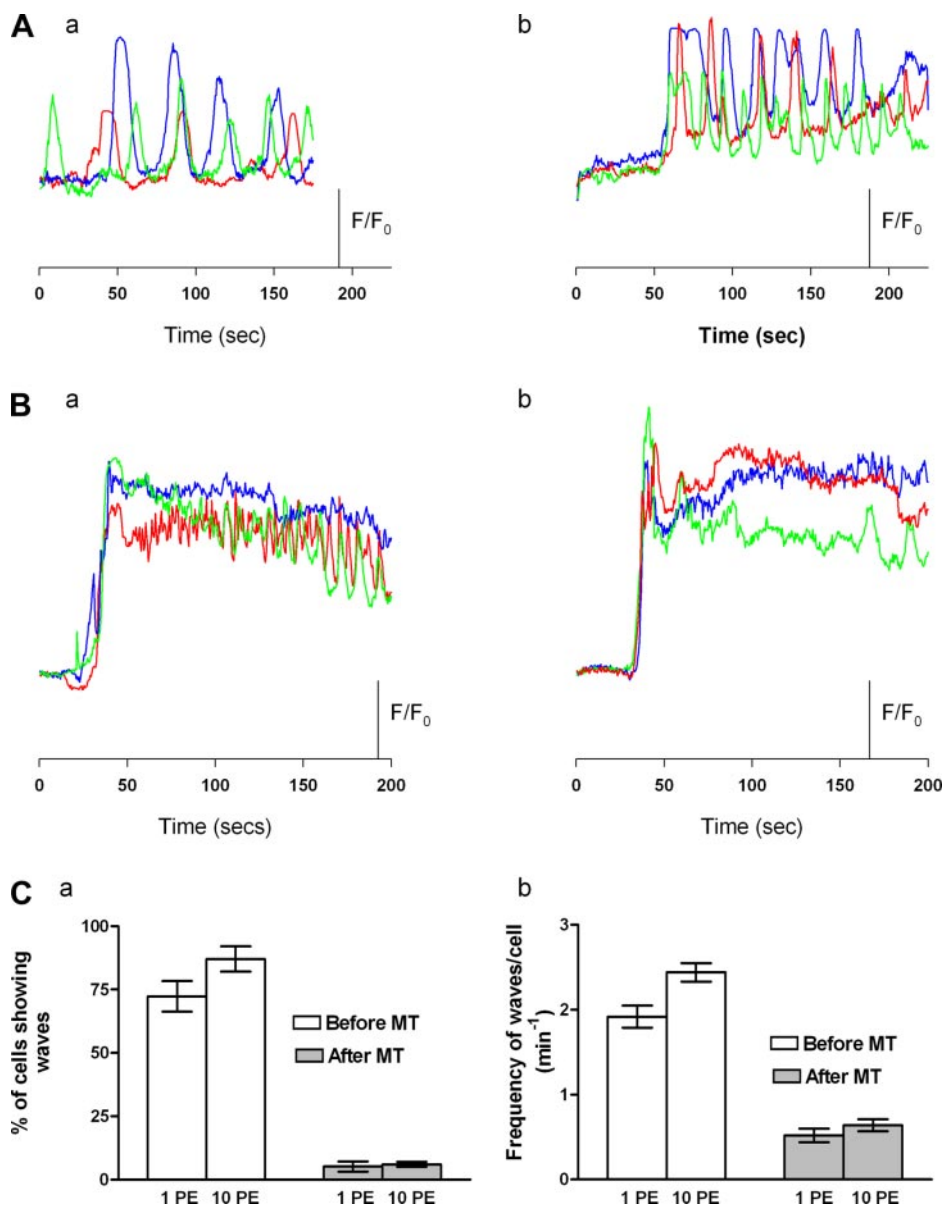


Fig. 4. α_1 -Adrenoceptor-induced Ca^{2+} signaling in individual SMCs of arteries consists of Ca^{2+} waves before MT and steady elevated Ca^{2+} after MT. *A*: Ca^{2+} signaling in response to PE at 1.0 μM (*a*) and 10.0 μM (*b*) in artery before MT had developed. *B*: Ca^{2+} signaling in response to PE at 1.0 μM (*a*) and 10.0 μM (*b*) in artery after MT had developed. Fluorescence calibration corresponds to 1.0 F/F_0 units. *C*: summarized data from 5 arteries in which the percentage of cells that showed at least 1 Ca^{2+} wave was calculated (*a*) and the average frequency of the waves is shown (*b*) (minimum number of waves, 2).

The usual response to PE was now a rapid increase in $[\text{Ca}^{2+}]$, followed by a sustained elevation (Fig. 4*B*). Over time, the elevated $[\text{Ca}^{2+}]$ tended to fall, and oscillations in $[\text{Ca}^{2+}]$ could then sometimes be evident (Fig. 4*Ba*, red and green trace). However, in five arteries with MT, PE (1.0 μM) elicited clear waves in only $5 \pm 2\%$ of the cells, and the average frequency of the waves was $0.52 \pm 0.08 \text{ min}^{-1}$ (Fig. 4*C*). At 10.0 μM , PE elicited waves in only $6 \pm 1\%$ of cells at an average frequency of $0.64 \pm 0.07 \text{ min}^{-1}$ (Fig. 4*C*). In cells in which steady elevated Ca^{2+} occurred, the fluorescence levels were $F/F_0 = 5.01 \pm 0.60$ ($n = 5$) in 113 cells at 1.0 μM PE and $F/F_0 = 6.11 \pm 0.72$ ($n = 5$) in 107 cells at 10.0 μM PE, respectively.

Thus α_1 -adrenoceptor-induced Ca^{2+} signaling in mouse mesenteric small arteries that have MT is markedly different from that in arteries that have not developed MT. The development and maintenance of MT involves a large number of signaling networks and ion channels, as well depolarization

and an increase in cytoplasmic $[\text{Ca}^{2+}]$. Therefore, we tested the possible involvement of some of these factors in the apparent modulation of α_1 -adrenoceptor-induced Ca^{2+} signaling by MT.

α_1 -Adrenoceptor-induced Ca^{2+} signaling in arteries with MT: possible role of elevated cytoplasmic $[\text{Ca}^{2+}]$. The elevated $[\text{Ca}^{2+}]$ that accompanies MT could possibly have many effects, including activation of PLC (leading to production of InsP_3), activation of conventional PKCs (e.g., $\text{PKC}\alpha$), and activation and inactivation of InsP_3Rs (depending on subtype). InsP_3Rs are particularly important in propagating asynchronous Ca^{2+} waves in smooth muscle, and therefore, any action of elevated Ca^{2+} to inactivate them might be particularly important in agonist-induced Ca^{2+} signaling.

To determine whether the differences in α_1 -adrenoceptor-induced Ca^{2+} signaling in arteries with and without MT might be related to the elevation of cytoplasmic $[\text{Ca}^{2+}]$ in the presence of MT, we examined α_1 -adrenoceptor-induced Ca^{2+}

signaling during alterations of cytoplasmic $[Ca^{2+}]$ in arteries that had and had not developed MT. In arteries that had not developed MT, PE (10.0 μ M) elicited propagating Ca^{2+} waves within individual SMCs, as described previously. Exposure to elevated external $[K^+]$ (25 mM) elevated cytoplasmic $[Ca^{2+}]$ (Fig. 5A). As judged by the change in F/F_0 , the increase in $[Ca^{2+}]$ was similar to that occurring during development of MT. A difference is that small cyclical oscillations in $[Ca^{2+}]$, of unknown mechanism, were typically present. In this condition, PE (10.0 μ M) further elevated cytoplasmic $[Ca^{2+}]$ but failed to elicit Ca^{2+} waves (Fig. 5B). The small oscillations disappeared as F/F_0 rose to very high levels (i.e., ~ 4.5). We also performed the converse experiment, in which $[Ca^{2+}]$ was experimentally reduced from its high levels in arteries that had developed MT. In this experiment, cytoplasmic $[Ca^{2+}]$ was lowered by block of L-type Ca^{2+} channels (known to be an important source of Ca^{2+} influx that contributes to the elevated cytoplasmic $[Ca^{2+}]$ in MT). Nifedipine completely inhibited MT and dilated the artery to its original diameter. In this condition, a higher concentration of PE (30.0 μ M) was used to elicit contraction. In three arteries, PE (30.0 μ M) produced waves in $52 \pm 3\%$ of cells, and the mean frequency of the waves was $1.07 \pm 0.041 \text{ min}^{-1}$ (Fig. 5, C and E). Although exposure to nifedipine did restore agonist-induced Ca^{2+} waves

in arteries that had developed MT (Fig. 5, D and E), the waves did not appear to be identical to those that typically occur before MT (e.g., Fig. 4A).

Agents such as nifedipine reduce both cytoplasmic $[Ca^{2+}]$ and MT. Therefore, it was also of interest to determine whether agents that reduce MT without primarily affecting cytoplasmic $[Ca^{2+}]$ also are capable of modulating the α_1 -adrenoceptor-induced Ca^{2+} signaling. In this case, the conversion of α_1 -adrenoceptor-induced Ca^{2+} signaling from Ca^{2+} waves to the Ca^{2+} "plateau" type of signaling would involve some of the other numerous signaling pathways that are known to be involved in myogenic tone. We tested the possible involvement of RhoA/Rho kinase (ROCK) by examining the effects of the ROCK inhibitor Y-27632 on α_1 -adrenoceptor-induced Ca^{2+} signaling in arteries that had developed MT. Rho kinase inhibition strongly inhibits MT in cerebral arteries without decreasing cytoplasmic $[Ca^{2+}]$ (5). As shown in Fig. 5F and G, inhibition of ROCK with Y-27632 (1.0 μ M) failed to restore α_1 -adrenoceptor-induced Ca^{2+} waves.

DISCUSSION

Previous work has revealed that bath-applied α_1 -adrenoceptor agonists elicit either asynchronous propagating Ca^{2+} waves

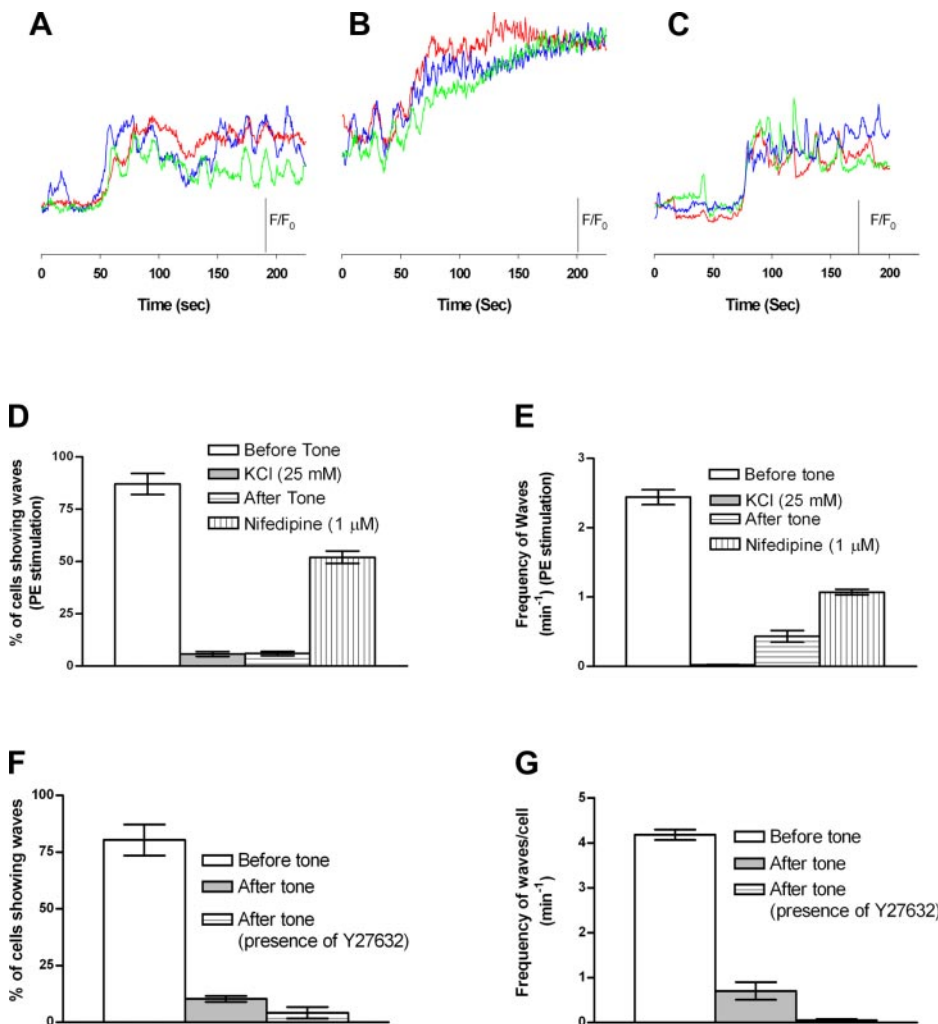


Fig. 5. Effects on α_1 -adrenoceptor-induced Ca^{2+} signaling of agents that affect intracellular $[Ca^{2+}]$ and/or MT: external K^+ , nifedipine, and a Rho kinase inhibitor. *A*: in 4 arteries that had not developed MT, KCl (25 mM) induced an increase in intracellular $[Ca^{2+}]$ accompanied by small, cyclical oscillations in $[Ca^{2+}]$ of unknown mechanism. *B*: after exposure to elevated $[K^+]$ (25 mM), however, PE (10 μ M) caused only steady elevated $[Ca^{2+}]$. *C*: in 3 different arteries that developed MT and were then exposed to nifedipine (1 μ M) to lower intracellular $[Ca^{2+}]$ and MT, activation of α_1 -adrenoceptors (30 μ M PE) caused Ca^{2+} waves. Data summarized are bar graphs D–G. In response to PE, the percentage of cells producing Ca^{2+} waves (D) and the frequency of the waves (E) were high before MT (open bars) and in the presence of nifedipine (vertically striped bars) but low in the presence of MT alone (horizontally striped bars) and when $[Ca^{2+}]$ was elevated by KCl, even in arteries that had not previously developed MT (shaded bars). *F* and *G*: in response to PE, most cells in 3 arteries produced asynchronous waves (open bars). After MT developed in these arteries, the fraction of cells producing waves (F) and the frequency of the waves (G) were both reduced (shaded bars). Addition of Y-27632 did not change the PE-induced Ca^{2+} signaling (striped bars).

or synchronous Ca^{2+} oscillations within individual SMCs of small arteries and veins (Table 1). Examination of the cited studies reveals that in arteries, α_1 -adrenoceptor agonists invariably (irrespective of temperature) activate Ca^{2+} waves if the artery is mounted isometrically, whether in a confocal wire myograph, stretched over a glass tube or pinned out. Similarly, Ca^{2+} waves or Ca^{2+} oscillations are invariably activated if the artery is mounted isobarically (e.g., pressurized at 70 mmHg) but studied at room temperature. Neither of these conditions (viz. isometric, room temperature) generally permits development of MT and the increase in cytosolic $[Ca^{2+}]$ that accompanies it. Adrenergic contractile activation of veins also has been studied extensively and appears exclusively to involve asynchronous Ca^{2+} waves (e.g., 31, 19, 21), with the exception of human saphenous vein (which generates a unique, only transient change in Ca^{2+} in response to PE) (2). The major finding of the present study, however, is that in mouse mesenteric small arteries, bath-applied α_1 -adrenoceptor agonists also may elicit a fundamentally different type of Ca^{2+} signal: a simple, spatially uniform, relatively constant increase in cytoplasmic $[Ca^{2+}]$. We refer to this as the plateau type of Ca^{2+} signal. Furthermore, we show that the cells of a given artery may produce either Ca^{2+} waves or a plateau, depending on whether or not cytoplasmic $[Ca^{2+}]$ is elevated to levels typical of fully developed MT. Thus the determinant seems not to be temperature or pressure, per se, but whether or not cytoplasmic $[Ca^{2+}]$ is elevated as a result of Ca^{2+} entry through voltage-dependent Ca^{2+} channels or other channels. Since MT, generated in part by intracellular $[Ca^{2+}]$, is expected to be present normally in mesenteric arteries of the intact animal, Ca^{2+} plateau in response to α_1 -adrenoceptor activation may be the most physiologically relevant type of adrenergic Ca^{2+} signal.

We assume that when they occur, Ca^{2+} oscillations in mouse mesenteric small arteries are critically dependent on

InsP₃R, just as they are in mesenteric arteries of the rat (16). Such cytoplasmic $[Ca^{2+}]$ oscillations must involve periodic increases and decreases of Ca^{2+} flux through InsP₃R, with increases likely resulting from the allosteric activation of InsP₃R by both cytoplasmic Ca^{2+} and InsP₃R and decreases resulting from one more possible mechanisms including 1) store depletion, 2) intrinsic inactivation of InsP₃R, and 3) Ca^{2+} -dependent inactivation of InsP₃R. Evidence also has been obtained that $[InsP_3]$ itself may oscillate, providing, in theory, oscillatory activation without the need for inactivation of InsP₃R.

A particularly appealing idea is that it is the Ca influx through L-type Ca^{2+} channels that is essential for inactivation of type 1 InsP₃R. Nevertheless, the existing data are equivocal: Ca^{2+} entry through voltage-gated Ca^{2+} channels either inhibits InsP₃-induced Ca^{2+} release (Ref. 14, in cerebellar neurons) or facilitates it (Ref. 34, in cortical neurons). Stutzmann et al. (34) suggests differences could be due to geometrical relationships of InsP₃R and L-type Ca^{2+} channels.

The present work has shown that before MT develops, a relatively small fraction of the SMCs within the wall of the pressurized artery are producing Ca^{2+} fluctuations, including large Ca^{2+} waves similar to those activated by α_1 -adrenoceptor agonists, as well as smaller fluctuations in $[Ca^{2+}]$ of unknown origin (Fig. 2Ba, blue trace). These Ca^{2+} transients do not seem to be associated with significant contraction, although Ca^{2+} waves induced by agonist at that time are, nevertheless, clearly associated with large vasoconstriction. The explanation may be that agonists activate a much larger fraction of the cells than are active spontaneously.

When MT develops spontaneously, $[Ca^{2+}]$ rises substantially in the individual cells, but not in all at the same time. Eventually, however, asynchronous propagating Ca^{2+} waves do largely disappear (possibly due to inactivation of InsP₃R, as

Table 1. Patterns of agonist-induced Ca^{2+} signals in vascular smooth muscle

Ref.	Tissue, Species	Agonist	Async	Sync	Plateau	MT, %	Temp, °C	Isobaric Pressure, mmHg	Isometric Conditions*
36	Mes art; rat	PE	+	–	–		21		Yes
24	Mes art; rat	PE	+	+	–	38	37	70	
8	Caudal art; rat	NE, EFS	+	–	–		30		Yes
1	Caudal art; rat	NE	+	–	–		37		Yes
13	Caudal art; rat	ACh, EFS	–	–	–		30		Yes
3	Caudal art; rat	Caff, NE	+	–	–		35		Yes
11	Cerebral art.; rat	UTP, KCl	+	–	–		22		Yes
10	Cerebral art.; rat	KCl	+	–	–	?	37	10–60	
16	Mes art; rat	Caff, PE	+	+	–	?	23	70	
20	IVC; rabbit	PE	+	–	–		22/37		Yes
23	Mes art; rat	PE	+	+	–		22	70	
2	Saph. vein; human	PE	–	–	–		37		Yes
19	IVC; rabbit	PE	+	–	–		37		Yes
28	Mes art; rat	NE	+	+	–		22/37		Yes
30	IVC; rabbit	PE, Caff	+	+	–		37		Yes
17	Mes art; rat	EFS	+	–	–		23		Yes
12	Mes art; mouse	PE	–	–	+	≈20	33	70	
29	Airway & pulm. arteriole; rat	5-HT, KCl	+	–	–		37		Yes
33	Mes art; rat	PE, U46619	+	–	–	?	37	50	
32	Mes art; rat	PE, U46619	+	+	–	?	37	50	
31	Mes art; rat	NE	+	+	–		34		Yes
Present	Mes art; mouse	PE	+	–	–	0	32	70	
Present	Mes art; mouse	PE	–	–	+	20	32	70	

Mes art, mesenteric artery; IVC, inferior vena cava; saph vein, saphenous vein; pulm., pulmonary; async, asynchronous calcium waves; Sync, synchronous calcium waves; plateau, calcium plateau; MT, myogenic tone; Temp, temperature; PE, phenylephrine; NE, norepinephrine; ACh, acetylcholine; Caff, caffeine; EFS, electrical field stimulation. *Includes 3 types of isometric studies: 1) stretched over a glass cannula, 2) wire myograph, and 3) pinned preparations.

discussed above), leaving either quiescent cells or those producing small Ca^{2+} ripples. The phenomenon shown in Fig. 2Bb (viz. large differences in $[\text{Ca}^{2+}]$ in different cells) would not be expected if all SMCs are well coupled electrically to each other and if the membrane potential of all the SMCs is synchronously depolarizing (promoting voltage-dependent Ca^{2+} entry through L-type Ca^{2+} channels). On the other hand, such a phenomenon might occur if clusters of L-type Ca^{2+} channels were also being activated by PKC (25), as well as by depolarization, but at different rates or times in different cells. It is already well established that PKC is activated during development of MT, playing an important role in the increased “ Ca^{2+} sensitivity” of contraction that is characteristic of MT.

The results and conclusions of the present study seem to differ from those of a previous study on the regulation of local and global Ca^{2+} signaling in cerebral artery SMCs (10). Previously, it was concluded that elevation of intravascular pressure induced propagating Ca^{2+} waves that were dependent on ryanodine receptors and that, together with Ca^{2+} sparks, had the effect of opposing vasoconstriction. Conclusive determination of the role of Ca^{2+} waves in activating contraction may await direct observation of MLCK, as has been done with carbachol-induced elevation of Ca^{2+} in mouse bladder SMCs (9).

In mesenteric arteries, asynchronous Ca^{2+} waves appear to activate contraction very effectively (Table 1). As speculated previously (18, 19), this may be due to the fact that Ca^{2+} released from the sarcoplasmic reticulum through InsP_3Rs is close to tethered calmodulin and MLCK. The source of the Ca^{2+} that gives rise to the plateau type of Ca^{2+} transients seen in the present study in arteries with MT is presently unknown. If, however, InsP_3R are inactivated in this condition, then surface membrane Ca^{2+} channels (L-type Ca^{2+} channels and/or receptor-operated channels) most likely are the source. These may deliver Ca^{2+} less effectively to the myofilaments, since the subplasmalemmal space is “myofilament poor” (19). This effect may be countered, however, by the well-known actions of both α_1 -adrenoceptors and intraluminal pressure to increase Ca^{2+} sensitivity of the myofilaments, particularly via inhibition of myosin light chain phosphatase through phosphorylation by Rho kinase (5). Remarkably, the net result under the near-physiological conditions we have used in this study is that agonist-induced vasoconstriction seems to be “adjusted” for existing vasoconstriction due to pressure (i.e., MT), since agonist-induced vasoconstriction tends to reach the same level regardless of whether MT is present or not (Fig. 1).

GRANTS

This work was supported by National Heart, Lung, and Blood Institute Grants HL-64708 [to W. G. Wier, principal investigator (PI)], HL-078870 (Project 3; to PI W. G. Wier), HL-45215 (to PI M. P. Blaustein), and HL-78870 (to PI M. P. Blaustein).

REFERENCES

- Asada Y, Yamazawa T, Hirose K, Takasaka T, Iino M. Dynamic Ca^{2+} signalling in rat arterial smooth muscle cells under the control of local renin-angiotensin system. *J Physiol* 521: 497–505, 1999.
- Crowley CM, Lee CH, Gin SA, Keep AM, Cook RC, van Breemen C. The mechanism of excitation-contraction coupling in phenylephrine-stimulated human saphenous vein. *Am J Physiol Heart Circ Physiol* 283: H1271–H1281, 2002.
- Dreja K, Nordstrom I, Hellstrand P. Rat arterial smooth muscle devoid of ryanodine receptor function; effects on cellular Ca^{2+} handling. *Br J Pharmacol* 132: 1957–1966, 2001.

- Duling BR, Gore RW, Dacey RG, Damon DN. Methods for isolation, cannulation and in vitro study of single microvessels. *Am J Physiol Heart Circ Physiol* 241: H108–H116, 1981.
- Gokina NI, Park KM, McElroy-Yaggy K, Osol G. Effects of Rho kinase inhibition on cerebral artery myogenic tone and reactivity. *J Appl Physiol* 98: 1940–1948, 2005.
- Haddock RE, Hill CE. Rhythmicity in arterial smooth muscle cells. *J Physiol* 566: 645–656, 2005.
- Hill MA, Zou H, Potocnik SJ, Meininger GA, Davis MJ. Arteriolar smooth muscle mechanotransduction: Ca^{2+} signaling pathways underlying myogenic reactivity. *J Appl Physiol* 91: 973–983, 2001.
- Iino M, Kasai H, Yamazawa T. Visualization of neural control of intracellular Ca^{2+} concentration in single vascular smooth muscle cell in situ. *EMBO J* 13: 5026–5031, 1994.
- Isotani E, Zhi G, Lau KS, Huang J, Mizuno Y, Persechini A, Geguchadze R, Kamm KE, Stull JT. Real-time evaluation of myosin light chain kinase activation in smooth muscle tissues from a transgenic calmodulin-biosensor mouse. *Proc Natl Acad Sci USA* 101: 6279–6284, 2004.
- Jaggard JH. Intravascular pressure regulates local and global Ca^{2+} signaling in cerebral artery smooth muscle cells. *Am J Physiol Cell Physiol* 281: C439–C448, 2001.
- Jaggard JH, Nelson MT. Differential regulation of Ca^{2+} sparks and Ca^{2+} waves by UTP in rat cerebral artery smooth muscle cells. *Am J Physiol Cell Physiol* 279: C1528–C1539, 2000.
- Ji G, Feldman ME, Deng KY, Greene KS, Wilson J, Lee JC, Johnston RC, Rishniw M, Tallini Y, Zhang J, Wier WG, Blaustein MP, Xin HB, Nakai J, Kotlikoff MI. Ca^{2+} -sensing transgenic mice: postsynaptic signaling in smooth muscle. *J Biol Chem* 279: 21461–21468, 2004.
- Kasai Y, Yamazawa T, Sakurai T, Taketani Y, Iino M. Endothelium-dependent frequency modulation of Ca^{2+} signaling in individual vascular smooth muscle cells of the rat. *J Physiol* 504: 349–357, 1998.
- Khodakhah K, Ogden D. Functional heterogeneity of calcium release by inositol trisphosphate in single Purkinje neurones, cultured cerebellar astrocytes, and peripheral tissues. *Proc Natl Acad Sci USA* 90: 4976–4980, 1993.
- Knot HJ, Nelson MT. Regulation of arterial diameter and wall $[\text{Ca}^{2+}]$ in cerebral arteries of rat by membrane potential and intravascular pressure. *J Physiol* 508: 199–209, 1998.
- Lamont C, Wier WG. Different roles of ryanodine receptors and inositol (1,4,5)-trisphosphate receptors in adrenergically stimulated contractions of small arteries. *Am J Physiol Heart Circ Physiol* 287: H617–H625, 2004.
- Lamont C, Vainorius E, Wier WG. Purinergic and adrenergic Ca^{2+} transients during neurogenic contractions of rat mesenteric small arteries. *J Physiol* 549: 801–808, 2003.
- Lee CH, Kuo KH, Dai D, van Breemen C. Asynchronous calcium waves in smooth muscle cells. *Can J Physiol Pharmacol* 83: 733–741, 2005.
- Lee CH, Poburko D, Kuo KH, Seow CY, van Breemen C. Ca^{2+} oscillations, gradients, and homeostasis in vascular smooth muscle. *Am J Physiol Heart Circ Physiol* 282: H1571–H1583, 2002.
- Lee CH, Poburko D, Sahota P, Sandhu J, Ruehlmann DO, van Breemen C. The mechanism of phenylephrine-mediated $[\text{Ca}^{2+}]_i$ oscillations underlying tonic contraction in the rabbit inferior vena cava. *J Physiol* 534: 641–650, 2001.
- Lee CH, Rahimian R, Szado T, Sandhu J, Poburko D, Behra T, van Breemen C. Sequential opening of IP_3 -sensitive Ca^{2+} channels and SOC during α -adrenergic activation of rabbit vena cava. *Am J Physiol Heart Circ Physiol* 282: H1768–H1777, 2002.
- MacMillan D, Currie S, Bradley KN, Muire TC, McCarron JG. IP_3 -mediated Ca^{2+} increases do not involve the ryanodine receptor, but ryanodine receptor antagonists reduce IP_3 -mediated Ca^{2+} increases in guinea-pig colonic smooth muscle cells. *J Physiol* 569: 533–544, 2005.
- Mauban JRH, Lamont C, Balke CW, Wier WG. Adrenergic stimulation of rat resistance arteries affects Ca^{2+} sparks, Ca^{2+} waves, and Ca^{2+} oscillations. *Am J Physiol Heart Circ Physiol* 280: H2399–H2405, 2001.
- Miriel VA, Mauban JRH, Blaustein MP, Wier WG. Local and cellular Ca^{2+} transients in smooth muscle of pressurized rat resistance arteries during myogenic and agonist stimulation. *J Physiol* 518: 815–824, 1999.
- Navedo MF, Amberg GC, Nieves M, Molkenin JD, Santana LF. Mechanisms underlying heterogeneous Ca^{2+} sparklet activity in arterial smooth muscle. *J Gen Physiol* 127: 611–622, 2006.
- Nilsson H, Aalkjaer C. Vasomotion: mechanisms and physiological importance. *Mol Interv* 3: 79–89, 2003.

27. **Osol G, Brekke JF, McElroy-Yaggy K, Gokina NI.** Myogenic tone, reactivity, and forced dilatation: a three-phase model of in vitro arterial myogenic behavior. *Am J Physiol Heart Circ Physiol* 283: H2260–H2267, 2002.
28. **Peng H, Matchkov V, Ivarsen A, Aalkjaer C, Nilsson H.** Hypothesis for the initiation of vasomotion. *Circ Res* 88: 810–815, 2001.
29. **Perez JF, Sanderson MJ.** The contraction of smooth muscle cells of intrapulmonary arterioles is determined by the frequency of Ca^{2+} oscillations induced by 5-HT and KCl. *J Gen Physiol* 125: 555–567, 2005.
30. **Ruehlmann DO, Lee CH, Poburko D, van Breemen C.** Asynchronous Ca^{2+} waves in intact venous smooth muscle. *Circ Res* 86: E72–E79, 2000.
31. **Sell M, Boldt W, Markwardt F.** Desynchronising effect of the endothelium on intracellular Ca^{2+} concentration dynamics in vascular smooth muscle cells of rat mesenteric arteries. *Cell Calcium* 32: 105–120, 2002.
32. **Shaw L, O'Neill S, Jones CJ, Austin C, Taggart MJ.** Comparison of U46619-, endothelin-1- or phenylephrine-induced changes in cellular Ca^{2+} profiles and Ca^{2+} sensitisation of constriction of pressurised rat resistance arteries. *Br J Pharmacol* 141: 678–688, 2004.
33. **Shaw L, Sweeney MA, O'Neill SC, Jones CJ, Austin C, Taggart MJ.** Caveolae and sarcoplasmic reticular coupling in smooth muscle cells of pressurised arteries: the relevance for Ca^{2+} oscillations and tone. *Cardiovasc Res* 69: 825–835, 2006.
34. **Stutzmann GE, LaFerla FM, Parker I.** Ca^{2+} signaling in mouse cortical neurons studied by two-photon imaging and photoreleased inositol triphosphate. *J Neurosci* 23: 758–765, 2003.
35. **Wier WG, Morgan KG.** α_1 -Adrenergic signaling mechanisms in contraction of resistance arteries. *Rev Physiol Biochem Pharmacol* 150: 91–139, 2003.
36. **Zang WJ, Balke CW, Wier WG.** Graded α_1 -adrenoceptor activation of arteries involves recruitment of smooth muscle cells to produce “all or none” Ca^{2+} signals. *Cell Calcium* 29: 327–334, 2003.

